Applied Thermal Engineering 31 (2011) 3000–3008

Contents lists available at ScienceDirect

Applied Thermal Engineering

journal homepage: www.elsevier.com/locate/apthermeng

Parametric optimization study of a multi-burner flameless combustion furnace

B. Danon [a,b], E.-S. Cho [a,*], W. de Jong [a], D.J.E.M. Roekaerts [a,b]

[a] Energy Technology, 3ME Faculty, Delft University of Technology, The Netherlands
[b] Multi-Scale Physics, Faculty of Applied Sciences, Delft University of Technology, The Netherlands

ARTICLE INFO

Article history:
Received 18 February 2011
Accepted 24 May 2011
Available online 31 May 2011

Keywords:
Flameless combustion
Multi-burner furnace
Parametric study
Optimization
Emissions
Efficiency

ABSTRACT

A parametric study on a 300 kW_{th} furnace equipped with three pairs of regenerative flameless combustion burners has been performed. Each burner pair has a rated thermal power of 100 kW_{th} firing Dutch natural gas. The objective of the study was to optimize the furnace performance, i.e., to maximize the cooling tube efficiency and minimize the CO and NO emissions. In the study the following parameters were varied: the positions of the burners in the furnace (burner configuration), the firing mode (parallel and staggered), the excess air ratio (λ) and the cycle time (t_{cycle}). Also, the influence on the furnace performance of the jet momentum of the combustion air and the temperature uniformity in the furnace were studied.

It was concluded that staggered firing mode is disadvantageous, since it results in significantly higher NO emissions than parallel firing mode. Also, out of the five investigated burner configurations one has been exempted, since its cooling tube efficiency was significantly lower compared to the other configurations. Furthermore, a horizontal setup of the firing burners improves the cooling tube efficiency at a fixed temperature uniformity. Also, for the burner configurations with the firing burners positioned closer to the regenerating burners and further from the stack, the temperatures in the regenerators are higher, leading to higher combustion air preheat temperatures. The temperature in the regenerators was also influenced by the cycle time; higher cycle times leading to higher (peak) temperatures in the regenerators. Finally, this temperature in the regenerators was shown to be more decisive for the final amount of CO emitted than the excess air ratio or the jet momentum. In all experiments, due to differences in path length of the mean flow, higher CO emissions were measured in the flue gas from the regenerators compared to in the flue gas from the stack. These two trends in the CO emissions were not observed for the NO emissions.

© 2011 Elsevier Ltd. All rights reserved.

1. Introduction

Energy efficiency and clean combustion are two main issues in fossil fuel utilization. Control of nitrogen oxides (NO_x) has been a major issue in designing combustion systems, since NO_x plays a key role in acid rain formation and the generation of photochemical smog. Flameless combustion, also known as Flameless Oxidation (FLOX®) [1], High Temperature Air Combustion (HiTAC) [2] or Moderate or intense low-oxygen dilution (Mild) combustion [3], is a promising combustion technology capable of accomplishing the combination of high efficiency and low emissions. It is based on delayed mixing of fuel and oxidizer and high flue gas recirculation. High momentum injection of the separated fuel and air flows entrain the flue gas through internal recirculation, thus diluting the oxygen concentration in the combustion zone. This leads to a more distributed heat release rate of the chemical energy, avoiding high peak temperatures and reducing the thermal formation of NO [4].

Since the introduction of flameless combustion in the early nineties of the last century, many universities and research departments of industry have made efforts in experimentally investigating this new technology. These studies have been performed on many different scales, from small jet-in-hot-coflow setups up to full industrial size furnaces. However, before wide industrial application of this technology can be established, more in-depth knowledge of its behaviour in industrial scale environments needs to become available, especially in (regenerative) multi-burner systems. The most important previous experimental studies that include multi-burner regenerative systems are discussed below.

At the fall of the second millennium, a 200 kW_{th} HiTAC furnace has been commissioned at the Kungl Tekniska Högskolan, Stockholm,

* Corresponding author. Tel.: +31 15 2785542; fax: +31 15 278 2460.
E-mail address: e.s.cho@tudelft.nl (E.-S. Cho).

1359-4311/$ – see front matter © 2011 Elsevier Ltd. All rights reserved.
doi:10.1016/j.applthermaleng.2011.05.033

Sweden [5]. In the furnace two pairs of NFK-HRS-DF regenerative burners firing natural gas and LPG were installed [6]. The two pairs of regenerative burners could be operated in three different firing configurations and the performance of the furnace has been compared extensively for these firing configurations [7–9].

In 2002 an extensive research program was performed at the IFRF research station in IJmuiden, The Netherlands [10]. The heating source in the furnace was one pair of NFK-HRS-DL4 regenerative burners, with a maximal thermal input of 1000 kW_{th}. Several types of fuel were investigated (natural gas, coke oven gas), while the objectives of the experiments were to generate extensive experimental datasets for the development and validation of CFD simulations.

A third large research project on regenerative flameless combustion was performed on a 200 kW_{th} furnace at the Faculté Polytechnique de Mons, Belgium [11]. One autoregenerative REGEMAT burner firing natural gas was used as the heating source. A comparison of the experimental data with CFD simulations was the main objective. In particular the heat transfer, temperatures and NO_x concentrations were compared.

Furthermore, at the NKK steel corporation in Japan, a slab reheating furnace with four pairs of regenerative burners was successfully fired with the by-product gas of the steel making factory [12,13]. The total thermal power input was 2919 kW_{th} and the heat sink was a moving slab in the bottom of the furnace. Also here, the obtained results served as validation data for CFD simulations of the furnace.

As can be concluded, although the above mentioned experimental studies are performed on furnaces equipped with either single autoregenerative burners or multiple regenerative burner pairs, none of them investigated the influence of the positions of the burners. The positioning of the burners can have a large influence on the furnace performance, especially in a regenerative (transient) environment. Therefore, investigation of the influence of burner positioning, such as burner–burner or burner–stack interactions, is required.

In this paper results are presented of an experimental campaign on a furnace equipped with three pairs of regenerative flameless combustion burners. An important degree of freedom in the experiments was the positioning of the three burner pairs. The objective is to investigate and, where possible, optimize the multi-burner furnace performance for the variation of four parameters. These parameters are the burner configuration, the firing mode, the excess air ratio and the cycle time. The optimization of the furnace performance is defined as the maximization of the cooling tube efficiency and minimization of the CO and NO emissions.

2. Experimental setup

A furnace equipped with three pairs of regenerative flameless combustion burners has been designed, built and commissioned at Delft University of Technology. In Fig. 1 a sketch of the furnace is presented. Each pair of regenerative flameless combustion burners has a rated thermal power of 100 kW_{th}, thus 300 kW_{th} in total. The fuel fired is Dutch natural gas, which has a net (lower) calorific value of 31.669 MJ/m^3 and consists of around 81%-vol CH_4, 3%-vol C_2H_6, 1%-vol other higher hydrocarbons, 14%-vol N_2 and 1%-vol other inert gases [14]. The burners were manufactured by WS Wärmeprozesstechnik GmbH and are of the REGEMAT CD 200 B type. Each burner has four combustion air/flue gas nozzles ($d = 20$ mm) around a central fuel nozzle ($d = 12$ mm).

The burners can operate in two different modes, i.e., flame and flameless mode. In flame mode the air and fuel are mixed in the burner before injection and the mixture is injected through the air nozzles only. An electric spark igniter is used in flame mode for ignition. In flameless mode the combustion air is injected through the air nozzles and the fuel is injected separately through the fuel nozzle. In this mode no igniter is necessary because the temperature in the furnace is above the self-ignition temperature of the fuel/air mixture. During the heating up of the furnace the burners fire in flame mode. Once the temperature in the furnace exceeds 850 °C (which is above the self-ignition temperature of the fuel/air mixture) the burners switch to flameless firing mode automatically. In this paper only results from the burners firing in flameless mode are presented.

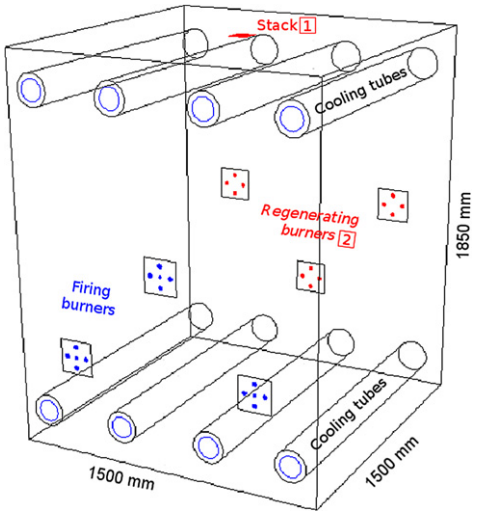

Fig. 1. Furnace sketch. The boxed numbers 1 and 2 indicate the two sample positions for the flue gas. Sampling point 2 is after the regenerators. All dimensions are in mm. The sketch represents burner configuration C5 firing in parallel mode (see also Table 1).

The furnace has inner dimensions of 1500 × 1500 × 1850 mm (length × width × height). The insulation consists of three layers of ceramic bricks, together 300 mm thick. During the experiments the wall temperature of the furnace was measured at various locations with slightly protruding thermocouples type S. Additionally, the temperature of the regenerated flue gases and the cooling air was measured with thermocouples type K. The measurement error of these thermocouples is around 2–5 K. One of these measurements, a double fitted thermocouple in the side wall close to the reaction zones, was determined to characterize the temperature in the furnace. Also, the temperature of the preheated air was measured in two burners (one burner pair). The fuel and combustion air flow rates are measured by custom-made orifice plate differential pressure meters. The combustion air flow rate is controlled by manual valves, allowing the variation of the excess air ratio.

Heat recirculation of the hot flue gases is achieved by regeneration. Eighty percent of the flue gases is sucked by a fan via the air nozzles of the regenerating burners over a ceramic honeycomb, while the remaining twenty percent leaves the furnace directly via the central stack at the roof. During regeneration the sucked flue gas traverses ceramic honeycomb heat exchangers situated inside the burners. The regenerated flue gas volume flow is measured using a vortex flow meter. The inlet temperature is between 800 and 900 °C and the outlet temperature is between 110 and 140 °C, under steady state conditions.

The thermal load is simulated by a cooling system which consists of eight single-ended cooling tubes, four placed at the bottom of the furnace and four at the top. Every cooling tube consists of two concentric tubes; the cooling air enters the inner tube, turns at the end and flows back through the annulus between the two tubes. This design was made to minimize the temperature

gradients along the length of the outer tube, thus, creating an as uniform as possible heat extraction distribution. The cooling air flow is measured using thermal mass flow meters and its inlet and exit temperatures are measured with type K thermocouples.

Additionally, a Sick Maihak S710 gas analyzer monitors the flue gas composition in two positions, i.e., in the stack and after the regenerators, see also Fig. 1. Using NDIR the concentrations of the pollutants (CO and NO) are determined. The average error in these emission measurements is ±7 ppm. In the same positions the O_2 concentration is determined paramagnetically for normalization purposes, with an accuracy of around ± 0.4 %-vol. All the data are stored by a data acquisition system every second.

In total eighteen flanges for the burners are divided over two opposite sides of the furnace (nine each). In this way, it is possible to investigate different burner configurations in the furnace.

3. Experimental campaign

Many different parameters were varied. In Table 1 all different parameters and their variation are summarized. The 'burner configuration' is defined as the physical position of the burners. The 'firing mode' is defined as which burners form a firing-regenerating pair. In parallel mode three burners fire at the same side, while in staggered mode two burners fire at one side and one burner at the opposing side, see also Table 1. Finally, the 'cycle time' (t_{cycle}) is defined as the total time of a complete firing and regenerating period of one burner.

Table 1
Overview of experiments. Burner configuration depicted by two sidewalls of the furnace with burner flanges (large circles), with numbers 1 to 6 the positions of the burners and small circles denote the positions of the cooling tubes. In parallel firing mode burners 1-2-3 fire simultaneously while 4-5-6 regenerate, et vice versa. In staggered firing mode burners 1-3-5 are firing while 2-4-6 regenerate, et vice versa.

Burner configuration		Firing mode	Cycle time (sec)	Excess air ratio (−)
C1	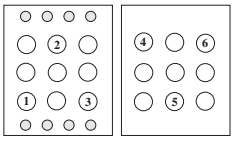	Parallel Staggered	20, 40, 60	1.05–1.35
C2	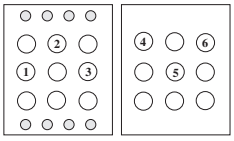	Parallel Staggered	20, 40, 60	1.05–1.35
C3	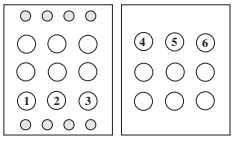	Parallel Staggered	20, 40, 60	1.05–1.35
C4	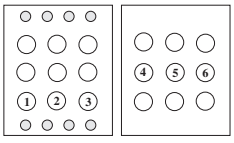	Parallel Staggered	20, 40, 60	1.05–1.35
C5	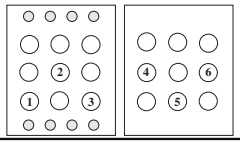	Parallel Staggered	20, 40, 60	1.05–1.35

The thermal performance of the furnace is characterized by the cooling tube efficiency, which is calculated by the difference in the sensible heat of the incoming and outflowing cooling air and its mass flow and subsequently divided by the total power input based on the net (lower) calorific value of the fuel.

The reported values of λ are a representation of the measured O_2 concentration in the flue gas from the stack. The O_2 concentration has been converted to λ with the following equation.

$$\lambda = \frac{20.9}{20.9 - [O_2]} \tag{1}$$

where $[O_2]$ is the molar oxygen percentage on dry basis.

The temperature uniformity is defined as in the following equation.

$$T_u = 1 - \sqrt{\frac{1}{N}\sum_{i=1}^{N}\left(\frac{(T_i - \overline{T})}{\overline{T}}\right)^2} \tag{2}$$

where N is the total number of temperature measurement positions, T_i is the temperature in the ith position and $\overline{T}$ is the mean of all the temperature measurements. The value of the T_u is between 0 and 1, where the value 1 indicates a perfectly uniform furnace. In the furnace the wall temperatures were measured with type S thermocouples in 18 different positions. Of these thermocouples, 12 are positioned in the unused burner flanges (see the empty circles in Table 1), while the remaining six are evenly divided over the other two side walls of the furnace.

The presented data are averages of a five to 10 min period of steady state operation and a round number of cycles.

4. Results and discussion

In this section the experimental results are discussed discriminated by the variation in the following parameters; the firing mode, the burner configuration, the excess air ratio (λ), the combustion air momentum, the cycle time (t_{cycle}) and the spatial temperature uniformity (T_u). For every parameter the influence on the cooling tube efficiency and the emissions are assessed.

Before proceeding to the parametric results, a remark is made on the emission measurements. In Fig. 2 the measured concentrations in the flue gas in the stack and from the regenerators are presented. The presented data is from configuration C3, but similar results were found for the other configurations. For these two flue gas sampling locations, see the boxed numbers in Fig. 1.

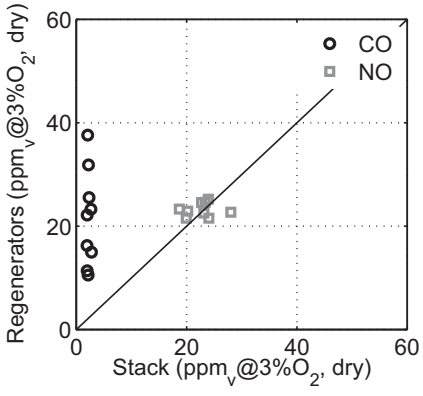

Fig. 2. Emission measurements (ppm$_v$@3%O_2, dry) in the flue gas from the stack and from the regenerators for burner configuration C3 firing in parallel mode.

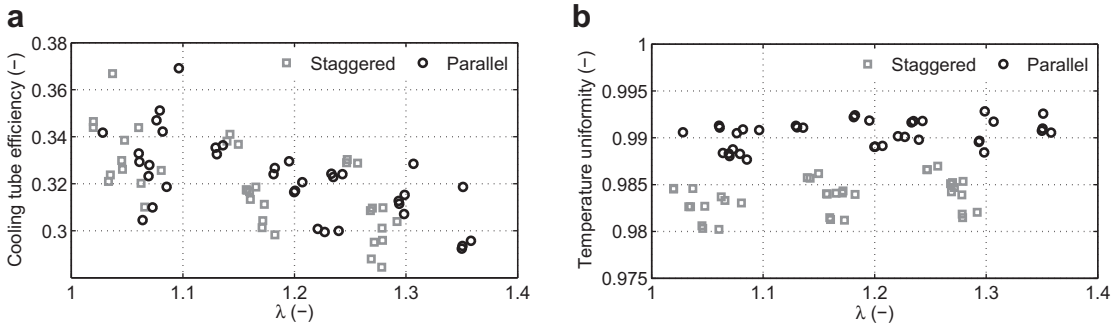

Fig. 3. (a) Cooling tube efficiency (−) and (b) temperature uniformity (−) for the different firing modes for all burner configurations, values of λ and cycle times.

The values of NO in both flue gas streams are comparable to each other and to values measured in other flameless combustion furnaces [8,10,15]. However, for the CO concentrations large differences are observed between the two flue gas streams. In the stack flue gas, no significant amounts of CO are detected, whereas in the regenerator flue gas small amounts of CO are detected. This is explained by the difference in pathlength of the mean flow; the pathlength of the mean flow of the gases from a firing burner is shorter to a regenerating burner compared to its pathlength to the stack. Due to the longer pathlength to the stack, more CO is allowed to be converted to CO_2 before leaving the furnace. It is concluded from these observations that the distance between the firing and regenerating burners in the present furnace is too short for the size of the burners.

In the parametric results below, the presented CO concentrations are the measured concentrations in the regenerator flue gas. The presented NO concentrations are the average of the measured concentrations of both flue gas streams.

4.1. Firing mode

In this section two different firing modes, i.e., parallel and staggered, are compared. For details about these firing modes see Table 1.

In Fig. 3(a) and (b) the cooling tube efficiency and the temperature uniformity are presented, respectively. Firstly, it is observed in Fig. 3(b) that in staggered firing mode the temperature in the furnace is less uniform compared to the cases firing in parallel mode. However, considering Fig. 3(a), these lower temperature uniformities do not result in lower cooling tube efficiencies. Actually, there are no significant differences in the cooling tube efficiency between the two firing modes.

It is noted here that the values of the cooling tube efficiency are lower than those of other furnaces, e.g., cooling tube efficiencies in KTH furnace are between 0.41 and 0.48 [9]. This is due to the fact that the burners in the KTH furnace use all the flue gases for regeneration, whereas the present burners use only 80%-wt of the flue gases for regeneration. The remaining 20%-wt of the flue gases is leaving the furnace at high temperature via the central stack.

In Fig. 4(a) and (b) the CO and NO emissions are compared, respectively. For the CO emissions, there are no significant differences between the two firing modes. However, it can be observed in Fig. 4(b), that the NO emissions in staggered mode are systematically higher than in parallel mode, for all the experiments. This difference in NO emissions for different firing modes has also been reported previously [7–9]. The increase in NO formation in staggered mode is caused by a shorter distance between the comburant nozzles and the point of confluence of the comburants. This shorter distance allows less flue gas to be entrained before the fuel and oxidizer mix [9].

It is concluded that in staggered firing mode, comparable cooling tube efficiencies are achieved as in parallel firing mode. However, regarding the emissions, staggered mode produces more NO at comparable thermal performance. Therefore, staggered firing mode is regarded as disadvantageous and is excluded from the following discussions.

4.2. Burner configuration

In Fig. 5 the cooling tube heat extraction rates for all the configurations are compared. It is shown that configuration C2 has a significantly lower cooling tube heat extraction compared to the other burner configurations. This is due to the fact that in configuration C2 all the burners are positioned in the upper two rows in the furnace, see also Table 1. Due to this fact, there are less flue gases flowing through the lower part of the furnace (note that the central stack is in the furnace roof), resulting in significant lower heat extraction by the lower cooling tubes. Based on these results it was decided to exclude configuration C2 from further investigation.

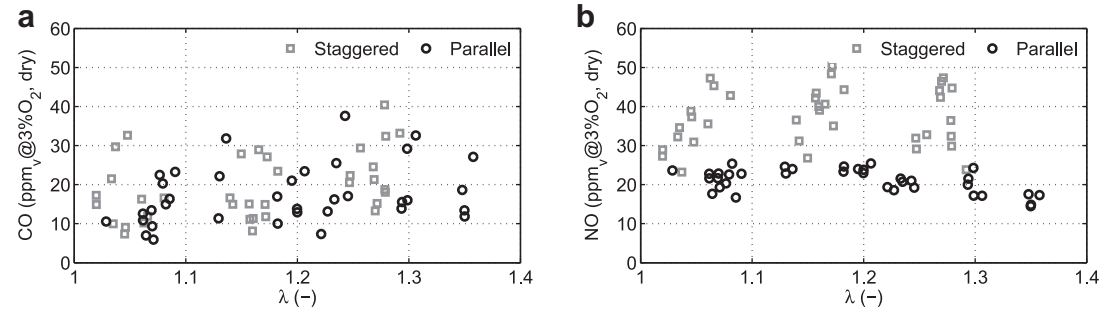

Fig. 4. (a) CO and (b) NO emissions ($ppm_v@3\%O_2$, dry) for the different firing modes for all burner configurations, values of λ and cycle times.

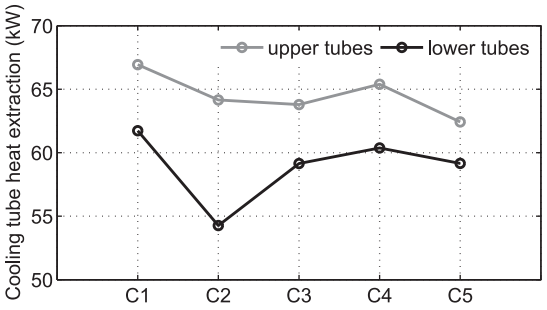

Fig. 5. Cooling tube heat extraction (kW) versus all burner configurations for parallel firing mode, $\lambda = 1.1$ and $t_{cycle} = 20$ s.

The increase in the combustion air flow also influences the regenerative preheating of the combustion air. In Fig. 6(a) in the previous section, it can be observed that for an increasing value of the λ, the preheat temperature of the combustion air is decreasing. As a result, also the exit temperature of the regenerated flue gas is lower, as shown in Fig. 6(b).

In Fig. 8(a) and (b) the CO and NO concentrations are presented for the C3 parallel experiment, respectively. The presented data is from configuration C3, but similar results were found for the other configurations. It is observed in (a) that higher values of λ causes slightly higher CO emissions. However, these differences are smaller than the effect of the cycle time, see for a discussion regarding the cycle time below. This unexpected trend of increasing CO emissions

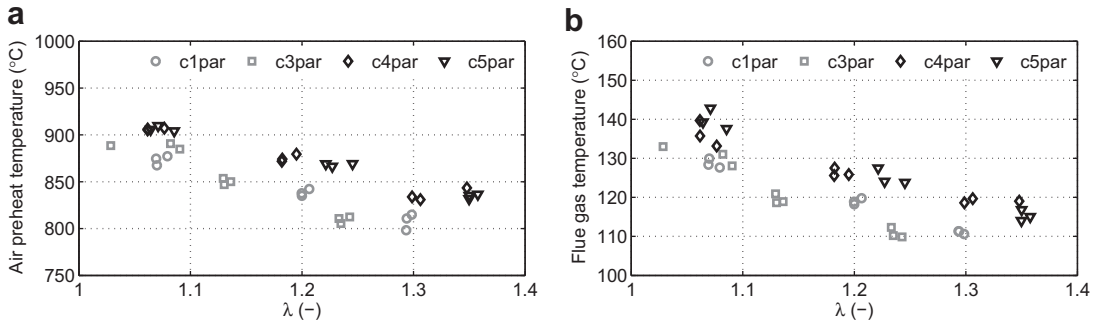

Fig. 6. (a) Combustion air preheat temperatures and (b) regenerated flue gas exit temperature (°C) for parallel firing mode and all values of λ and t_{cycle}.

In Fig. 6(a) and (b) the preheat temperature of the combustion air and the exit temperature of the regenerated flue gas are presented. A difference in these temperatures is observed for burner configurations C1 and C3 on the one hand, and configurations C4 and C5 on the other hand. The temperatures are consistently lower for C1 and C3, over the whole range of λ compared to C4 and C5. There are two explanations for the observed lower preheat and exit temperatures in configurations C1 and C3. In the first place, a shorter distance between the upper level burners and the stack in the roof in configurations C1 and C3, causes relatively more flue gas to flow towards the stack. This difference was confirmed by the measured values of the flue gas flow from the regenerators. Due to this burner–stack interaction, less flue gas is available for regeneration. Secondly, in these cases, the flue gases from a firing burner on the lower level, travelling to a regenerating burner on the higher level, have a longer pathlength, and thus a longer residence time in the furnace. This burner–burner interaction results in more heat exchange with the cooling tubes and furnace walls.

Finally, the differences in cooling tube efficiencies and CO and NO emissions between the other four burner configurations were too small compared to the influence of parameters that could not be controlled, such as the ambient temperature or the preheating time of the furnace, to draw solid conclusions.

4.3. Excess air ratio

In Fig. 7 the cooling tube efficiency is shown versus the excess air ratio λ for all burner configurations and cycle times. It is observed that the cooling tube efficiency shows a decreasing trend with increasing λ. This is explained by the fact that the increase in λ is achieved by increasing the combustion air mass flow, at constant fuel flow. Thus, more inert gases from the air (mainly N_2) are introduced in the furnace, resulting in a lower energy content per unit mass flue gas and thus lower efficiencies.

at increasing λ (a higher λ implies higher concentrations of O_2 and thus less CO) is explained by the temperatures of the combustion air and flue gas. As shown in Fig. 6(a) and (b), the air preheat temperature and regenerated flue gas exit temperature decrease with increasing λ. It is noted here that due to the increased combustion air mass flow at higher values of λ also the residence time will be shortened, however, these differences will be relatively small. Thus, two opposing effects are influencing the conversion of CO to CO_2; increased O_2 concentration is enhancing the reactions, whereas lower temperatures are slowing down the reactions. In these experiments the temperature has a stronger effect on the reactions, which is in accordance with what has been reported in the literature [16]. Finally, regarding Fig. 8(b), the NO emissions are not correlated to the value of λ, at least not within the investigated range.

In conclusion, considering both the cooling tube efficiency and the CO emissions, a value of λ closest to unity is optimal. It is noted here that the observed differences in the CO emissions are strongly related to the regenerative preheating of the combustion air.

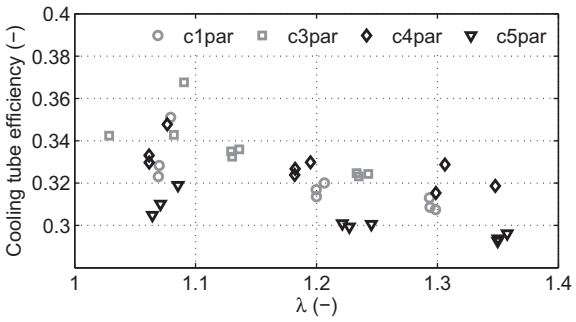

Fig. 7. Cooling tube efficiency (−) versus λ (−) for parallel firing mode and all burner configurations and cycle times.

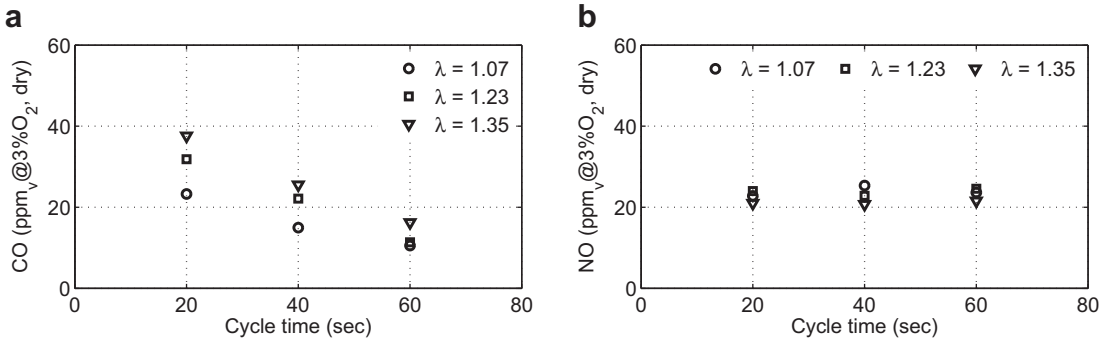

Fig. 8. (a) CO and (b) NO emissions (ppm$_v$@3%O_2, dry) versus the cycle time for C3 configuration in parallel firing mode, for all values of λ.

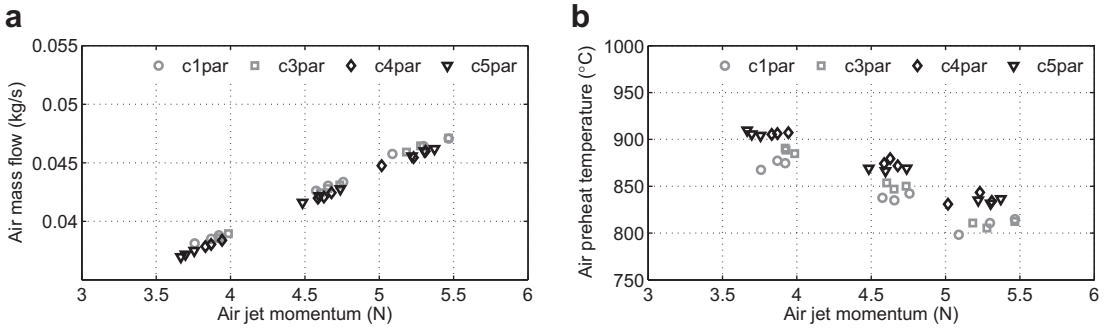

Fig. 9. Correlation between the combustion air jet momentum (N) and (a) the mass flow (kg/s) and (b) the preheat temperature (°C) of the combustion air for all configurations firing parallel mode and all values of λ and cycle time.

4.4. Combustion air momentum

In the literature it is mentioned that flameless combustion is achieved by high internal flue gas recirculation, which in turn is realized by discrete high momentum injection of the comburants [1,2]. The momentum of the combustion air jet is calculated by Equation (3).

$$G = \frac{RT\Phi_{\text{air}}^2}{pM_{\text{air}}A} \tag{3}$$

where G stands for jet momentum (N), Φ_{air} the mass flow of combustion air (kg/s), R is the universal gas constant (J/molK), T is the (preheat) temperature of the combustion air (K), p the pressure (Pa), M_{air} the molecular weight of air (kg/mol) and A the area of the air nozzles (m^2). Note that since the mass flow and temperature of the fuel jet are equal for all experiments the fuel jet momentum is also equal for all cases and the trends in the air jet momentum are equal to the trends in the momentum ratio. In these burners the average inlet velocity of the combustion air and fuel jets is around 100 and 30 ms^{-1}, respectively.

Firstly, the parameters influencing the jet momentum are discussed. In Fig. 9(a) and (b) the combustion air jet momentum is presented as a function of the air mass flow and the air preheat temperature. As expected from the equation, the jet momentum is increasing for increasing air mass flow. Contrarily, the air preheat temperature is decreasing with increasing air momentum, i.e., increasing air mass flow or λ. Thus, the air mass flow has a stronger influence on the jet momentum, which is confirmed in the equation, where the air mass flow is squared.

Secondly, the effect of the air jet momentum on the furnace performance is investigated. In Fig. 10 the cooling tube efficiency is presented versus the combustion air jet momentum. It is noted that the efficiency is decreasing for an increase in the jet momentum. This is in accordance with the trend observed for the cooling tube efficiency as a function of the λ, see also Fig. 7. Actually, in this case the trend is even more pronounced, since the jet momentum incorporates both the effects of the air mass flow, i.e., the λ, and the preheat temperature.

In Fig. 11(a) and (b) the emissions of CO and NO as a function of the jet momentum are presented, respectively. The CO emissions are increasing with an increasing jet momentum. Although an increasing jet momentum indicates increased oxygen concentration and increased internal flue gas recirculation (two effects enhancing the CO to CO_2 conversion), still the decrease in the air preheat temperature has the largest influence on this conversion. It is concluded that under flameless combustion conditions the preheat temperature of the air is an important parameter for the emission of CO.

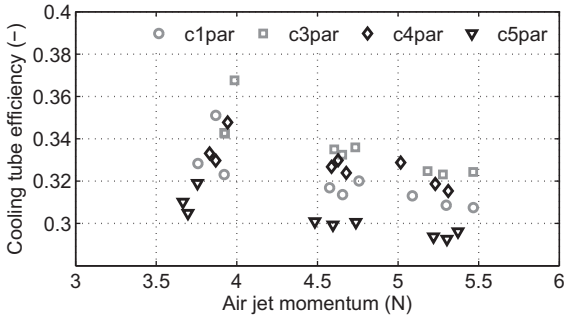

Fig. 10. Cooling tube efficiency (–) versus air jet momentum (N) for all configurations firing parallel mode and all values of λ and cycle time.

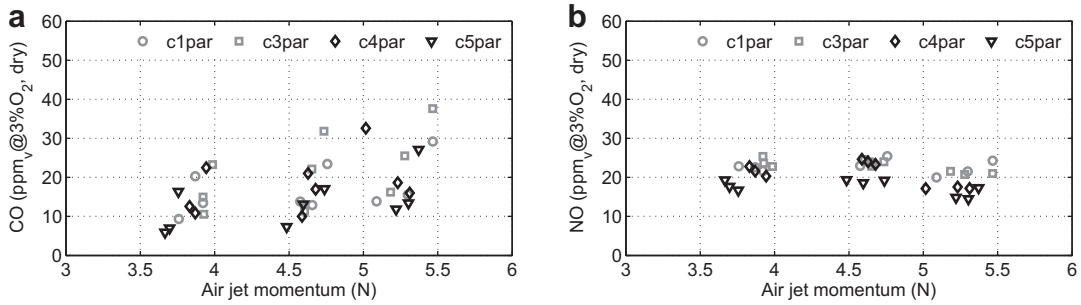

Fig. 11. (a) CO and (b) NO emissions ($ppm_v@3\%O_2$, dry) versus combustion air jet momentum (N) for all configurations firing parallel mode and all values of λ and cycle time.

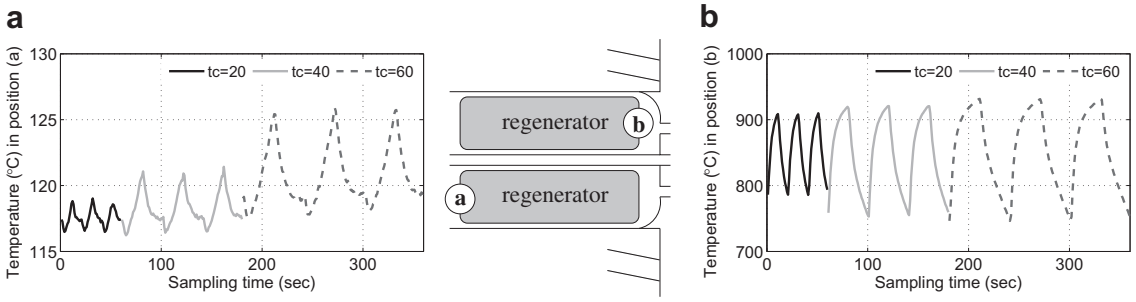

Fig. 12. Temperature (°C) at the cold side, position (a), and at the hot side, position (b), of the regenerator of one burner during configuration C3, parallel firing mode, $\lambda = 1.2$ and all cycle times. The actual measurement positions of Figures (a) and (b) are represented in the sketch of the burner by the encircled a and b, respectively. For every cycle time three entire cycles are presented, with the first half of the cycle a regenerating period.

The NO emissions show no significant correlation with respect to the jet momentum. Since the NO emission values are also low, it shows that the 'flamelessness' of the burners suppresses possible increases in the NO emissions due to the increase in preheat temperature or oxygen availability.

4.5. Cycle time

In Fig. 8(a) and (b) the CO and NO emissions are presented as a function of the cycle time for burner configuration C3, respectively. The NO emissions are not significantly affected by the change in cycle time. However, the CO emissions show a clear dependency with the cycle time; lower CO emissions are measured at longer cycle times.

This trend is due to the additional conversion of CO to CO_2 in the flue gas in the regenerators. Actually, the flue gas at the hot side of the regenerators has a temperature of around 850 °C, cf. the air preheat temperature, see also Fig. 6(a). At these temperatures the above mentioned reaction has significant rates [16].

In Fig. 12(a) and (b) the temperature at the cold and hot side of the regenerators of one burner are presented for a period of three entire cycles for all values of t_{cycle}. The presented data is from configuration C3, but similar results were found for the other configurations. It is noted here that the presented temperatures were measured in a burner that regenerates the first half of the cycle, and fires the second half. It is observed that in case of longer cycle times, the maximum temperature of the flue gas entering the regenerators, i.e., the first half of the cycles in (b), is higher and that this temperature is reached relatively faster. Also, the exit temperature of the flue gas is higher for longer cycle times, as can be seen in the first half of the cycles in (a). Thus, in the cases with longer cycle time, the flue gases cross the regenerators at higher temperatures and, relatively to the entire cycle time, for a longer time at these high temperatures. This explains the lower measured CO levels for longer cycle times.

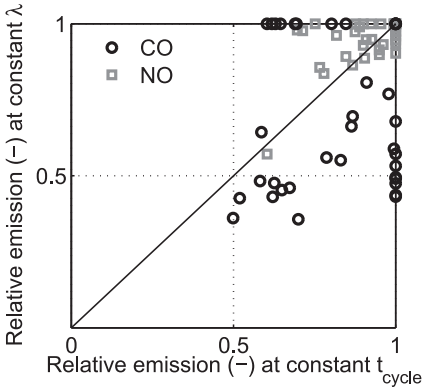

Fig. 13. Relative CO and NO emissions (−) at constant t_{cycle} and λ, for all burner configurations in parallel firing mode.

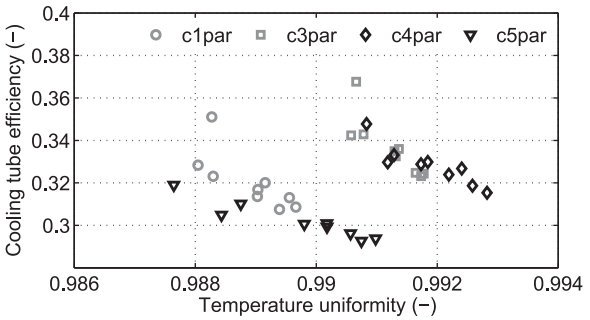

Fig. 14. Cooling tube efficiency (−) versus temperature uniformity (−) for all burner configurations in parallel firing mode and all values for λ and cycle time.

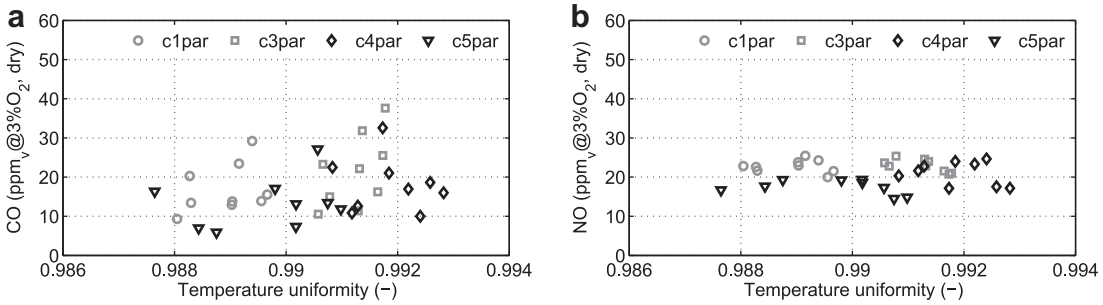

Fig. 15. (a) CO and (b) NO emissions (ppm_v@3%O_2, dry) versus the temperature uniformity (−) for all burner configurations in parallel firing mode and all cycle times and values for λ.

As a next step, the relative emissions of CO and NO, at a constant value for the λ and t_{cycle}, are calculated with Equation (4).

$$\text{Relative emission} = \left(\frac{x_i}{x_{i,\max}}\right)_j \tag{4}$$

where x_i is the mole fraction (−) of species i (either CO or NO) and j represents either at constant λ or t_{cycle}. Every case is part of a series obtained by variation of λ (and thus at constant t_{cycle}), and part of a series obtained by variation of the cycle time (and thus at constant λ). The relative emission is calculated twice for each case, i.e., as part of one of these two series. For all cases the two relative emissions are plotted versus each other in Fig. 13.

It is observed that the relative NO emissions are randomly scattered around the 'parity line', which indicates that none of the two effects (λ or t_{cycle}) has a significant larger influence than the other. Also, the values are close to unity, indicating that the differences in the NO emissions between the cases are small.

However, most of the CO relative emissions are below the 'parity line'. This clearly indicates that a change in the λ (along x-axis) has a smaller effect on the CO emissions than a change in the cycle time (along y-axis). In other words, while the cycle time has no effect on the NO emissions, it does effect the CO emissions, see also Fig. 8. Moreover, the effect of the cycle time on the CO emissions is larger than the effect of the λ.

Finally, the cooling tube efficiency showed no relation with the variation of the cycle time.

4.6. Temperature uniformity

In many publications it is reported that flameless combustion is achieving a more uniform temperature distribution compared to conventional combustion and that this higher temperature uniformity results in higher efficiencies [17,18].

To verify whether this hypothesis holds for different cases under flameless combustion conditions, the temperature uniformity is presented versus the cooling tube efficiency in Fig. 14. Note that a value of unity for the temperature uniformity represents perfect uniformity, whereas a decreasing value of the temperature uniformity indicates an increase in the temperature gradients in the furnace.

Considering the burner configurations separately, the cooling tube efficiency shows a decrease with increasing temperature uniformity. This contradicts the general validity of the above mentioned hypothesis.

Furthermore, it is observed that burner configurations C1 and C5 together tend to a linear correlation with the temperature uniformity, as configurations C3 and C4 do. In this view, a horizontal setup of the firing burners (C3 and C4) behaves differently from a triangular setup of the firing burners (C1 and C5, see Table 1). Additionally, the horizontal firing setup achieves higher cooling tube efficiencies, compared to the triangular firing setup, for the same values of the temperature uniformity. The same observation can be made in Fig. 10. Therefore, the observed trends in Fig. 14 are related to burner–burner interactions.

Finally, in Fig. 15(a) and (b) the CO and NO emissions are presented as a function of the temperature uniformity. For the formation of both pollutants no clear correlation with the temperature uniformity could be identified.

5. Conclusions

A parametric study has been performed on a multi-burner flameless combustion furnace with the objective of optimizing the furnace performance, i.e., maximizing the cooling tube efficiency and minimizing the emissions (CO and NO). From a first observation, regarding the difference in CO emissions in the flue gas from the regenerators and in the central stack, the present furnace is too small for the size of the burners.

For the optimization of the furnace performance, two conditions could be ruled out. First, staggered firing mode has been ruled out mainly due to higher NO emissions. Secondly, burner configuration C2 (see Table 1) was exempted, since the cooling tube efficiency was significantly lower compared to the other burner configurations.

Furthermore, it was observed that for burner configurations C4 and C5, with the burners positioned in the middle and lower levels in the furnace, the combustion air preheat and flue gas exit temperatures are higher than for burner configurations C1 and C3. However, this trend was not reflected in the CO emissions. Then, configurations C3 and C4, with a horizontal setup of the firing burners, showed better cooling tubes efficiencies than configurations C1 and C5, at comparable values of the temperature uniformity. It was also shown that with an increase in the λ, the cooling tube efficiency decreased. However, although both the oxygen availability and the internal flue gas recirculation are increased with an increasing λ, also the CO emissions increased. This was due to decreased temperatures in the regenerators. Finally, it was observed that for different cases under flameless combustion conditions, the cooling tube efficiency showed a decreasing trend with increasing temperature uniformities.

Although no distinct optimal case could be identified, some conditions could be exempted. Moreover, it was shown that the positioning of the burners, and thus the burner–burner and burner–stack interactions, influenced the performance of the furnace.

These experimental results will serve as validation data for a set of Computational Fluid Dynamics simulations of the furnace. The objective of these simulations will be the explanation of the currently presented results.

Acknowledgements

This project has been financially supported by the Dutch Technology Foundation (STW) and the Dutch Flame Foundation (NVV).

References

[1] J. Wünning, J. Wünning, Flameless oxidation to reduce thermal NO-formation, Progress in Energy and Combustion Science 23 (1997) 81–94.
[2] H. Tsuji, A. Gupta, T. Hasegawa, M. Katsuki, K. Kishimoto, M. Morita, High Temperature Air Combustion: From Energy Conservation to Pollution Reduction. CRC Press, 2003.
[3] A. Cavaliere, M. de Joannon, Mild combustion, Progress in Energy and Combustion Science 30 (2004) 329–366.
[4] J. Miller, C. Bowman, Mechanism and modeling of nitrogen chemistry in combustion, Progress in Energy and Combustion Science 15 (1989) 287–338.
[5] W. Blasiak, T. Dobski, S. Lille, M. Mörtberg, N. Rafidi, Combustion tests in a test furnace equipped with high temperature air combustion mode, in: Proceedings of the 4th High Temperature Air and Gasification Conference (HTACG). Rome, Italy (2001).
[6] W. Blasiak, W. Yang, N. Rafidi, Physical properties of a LPG flame with high-temperature air on a regenerative burner, Combustion and Flame 136 (2004) 567–569.
[7] W. Yang, M. Mörtberg, W. Blasiak, Influence of flame configurations on flame properties and NO emissions in combustion with high-temperature air, Scandinavian Journal of Metallurgy 34 (2005) 7–15.
[8] N. Rafidi, W. Blasiak, Heat transfer characteristics of HiTAC heating furnace using regenerative burners, Applied Thermal Engineering 26 (2006) 2027–2034.
[9] B. Danon, A. Swiderski, W. de Jong, W. Yang, D. Roekaerts, Emission and efficiency comparison of different firing modes in a furnace with four HiTAC burners, Combustion Science and Technology 183 (7) (2011) 686–703.
[10] B. Burggraaf, B. Lewis, P. Hoppesteyn, N. Fricker, S. Santos, B. Slim, Towards industrial application of high efficiency combustion, IFRF Combustion Journal (2007) 200704.
[11] D. Lupant, B. Pesenti, P. Evrard, P. Lybaert, Numerical and experimental characterization of a self-regenerative flameless oxidation burner operation in a pilot-scale furnace, Combustion Science and Technology 179 (2007) 437–453.
[12] C. Zhang, T. Ishii, Y. Hino, S. Sugiyama, The numerical and experimental study of non-premixed combustion flames in regenerative furnaces, Journal of Heat Transfer 122 (2000) 287–293.
[13] T. Ishii, C. Zhang, Y. Hino, Numerical study of the performance of a regenerative furnace, Heat Transfer Engineering 23 (2002) 23–33.
[14] Physical Properties of Natural Gases. Nederlandse Gasunie N.V, 1980.
[15] D. Lupant, B. Pesenti, P. Lybaert, Detailed characterization of flameless oxidation on a laboratory scale furnace. in: G. Skevis (Ed.), Proceedings of the 3rd European Combustion Meeting. Chania, Greece (2007).
[16] D. Baulch, D. Drysale, An evaluation of the rate data for the reaction $CO+OH \rightarrow CO_2+H$, Combustion and Flame 23 (1974) 215–225.
[17] F. Christo, B. Dally, Modeling turbulent reacting jets issuing into a hot and diluted coflow, Combustion and Flame 142 (2005) 117–129.
[18] R. Weber, J. Smart, W. van de Kamp, On the MILD combustion of gaseous, liquid, and solid fuels in high temperature preheated air, Proceedings of the Combustion Institute 30 (2005) 2623–2629.